

Supporting Information

**Visible light Photo-oxidation of Model Pollutants Using
CaCu₃Ti₄O₁₂: An Experimental and Theoretical Study of
Optical Properties, Electronic Structure and properties,
electronic structure and selectivity**

Joanna H. Clark, Matthew S. Dyer, Robert G. Palgrave, Christopher P. Ireland, James R. Darwent, John B. Claridge, Matthew J. Rosseinsky

Department of Chemistry, University of Liverpool, Liverpool, L69 7ZD, United Kingdom

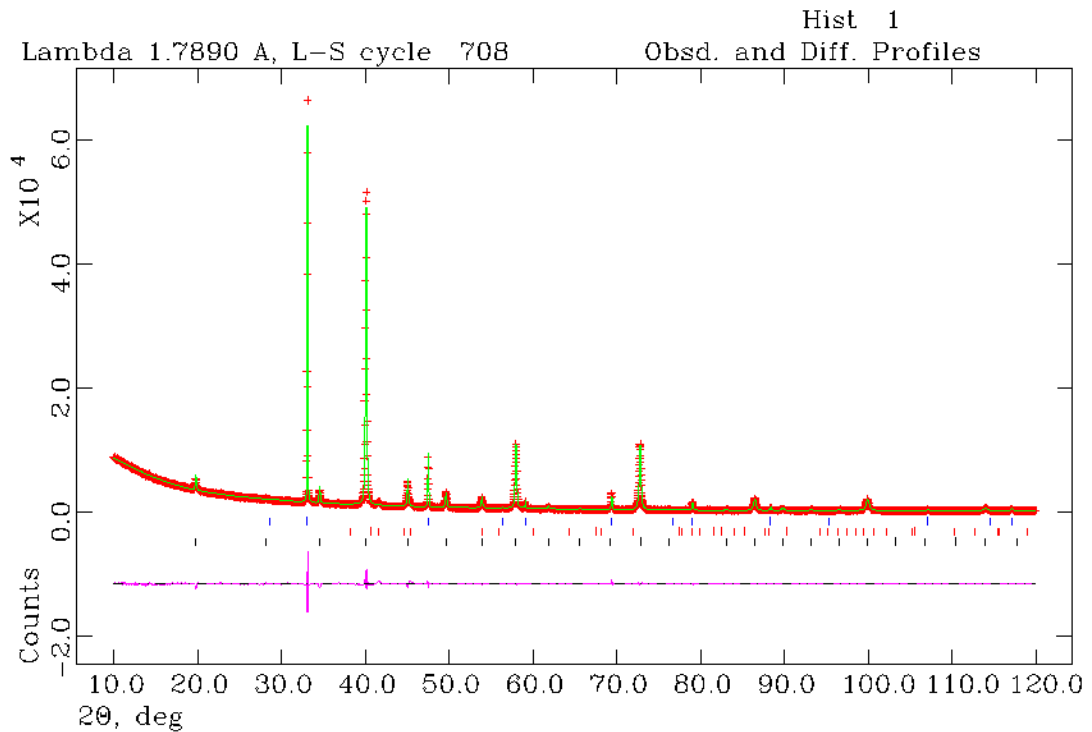


Figure S1. Observed, calculated and difference plots for the 3 phase structural refinement of sol-gel derived $\text{CaCu}_3\text{Ti}_4\text{O}_{12}$ (OA 1:1:1) with CuO impurity (estimated at <2% of sample) and KCl as an internal standard. $\text{Im } \bar{3} \text{ } a=7.39463\text{\AA}$. Final goodness-of-fit parameters: $\text{Rp}=2.86\%$, $\text{wRp}=4.50\%$, $\chi^2=3.186$.

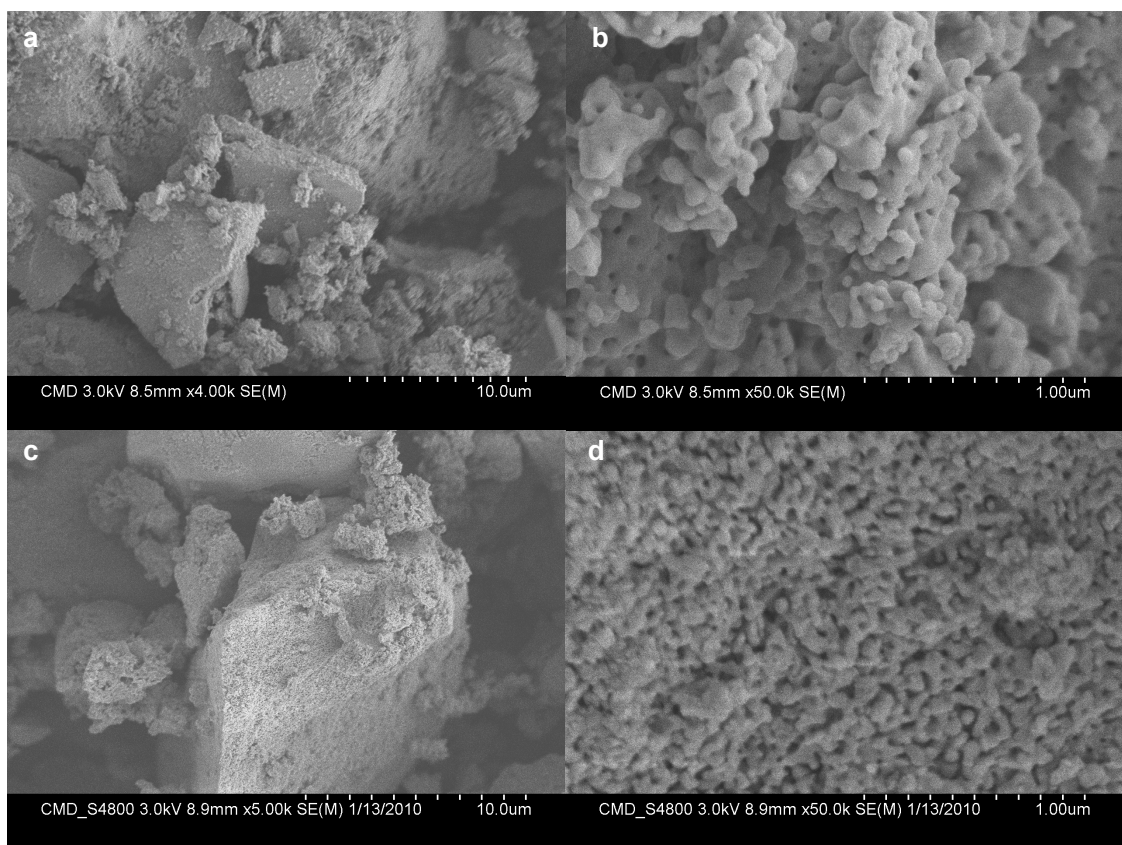


Figure S2. SEM images of Pt-CaCu₃Ti₄O₁₂ (OA 1:1:1, pH1) before (a and b) and after (c and d) testing for activity toward photo-oxidation of MO

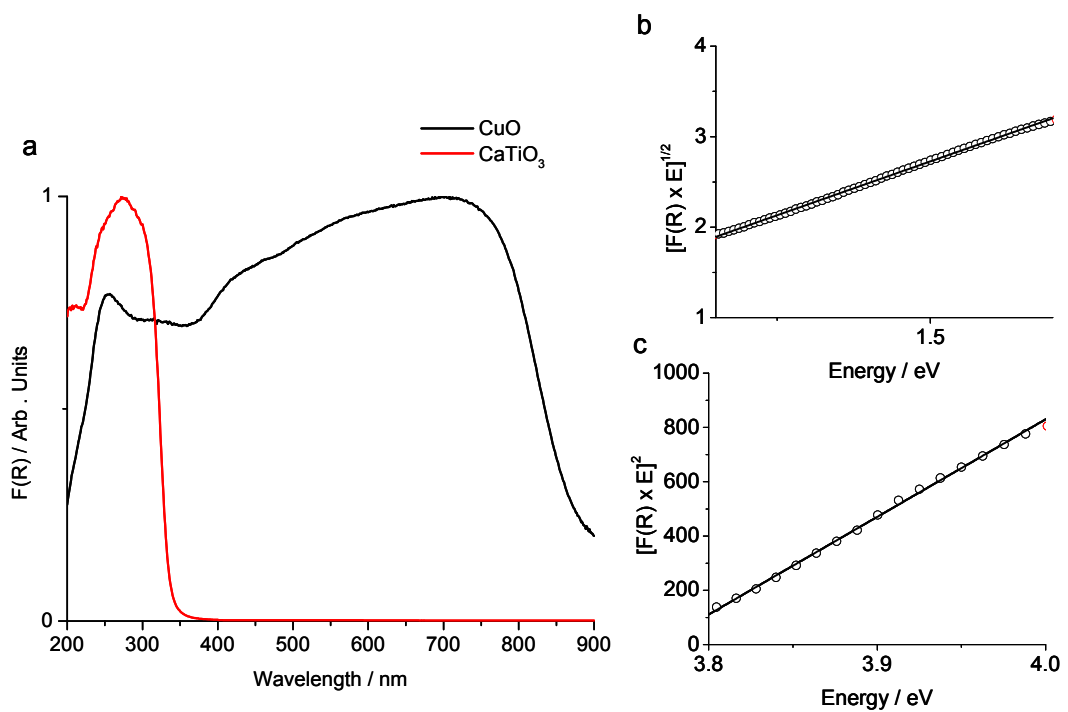


Figure S3. Diffuse reflectance spectra of CuO and CaTiO₃, and linear fittings of absorption edges of
b) CuO to an indirect transition of 1.27eV and c) CaTiO₃ to a direct transition of 3.76eV.

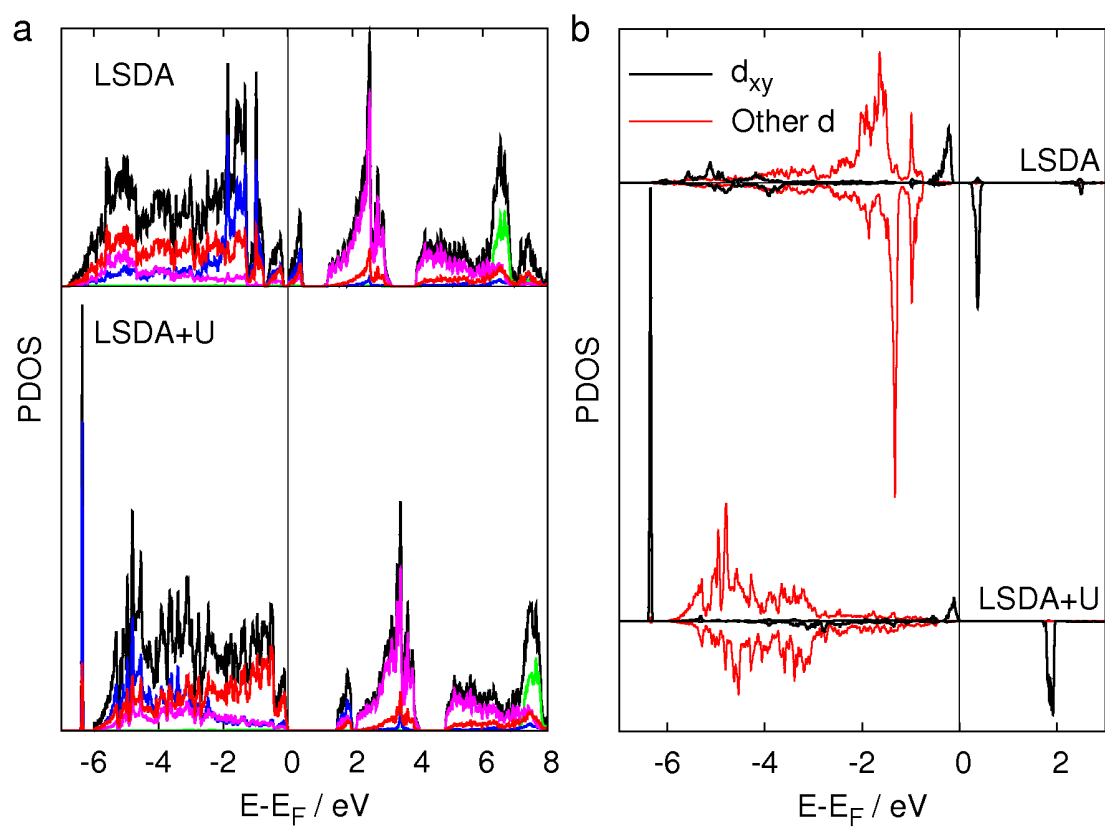


Figure S4.a) Total and partial density of states (PDOS) calculated using LSDA and LSDA+U. The PDOS is projected onto the Ca, Cu, Ti and O atoms. **b)** PDOS projected onto the d_{xy} orbital and the sum of the remaining d_{xz} , d_{yz} , d_{z^2} and $d_{x^2-y^2}$ orbitals of the Cu atom coordinated to O atoms in the xy plane.

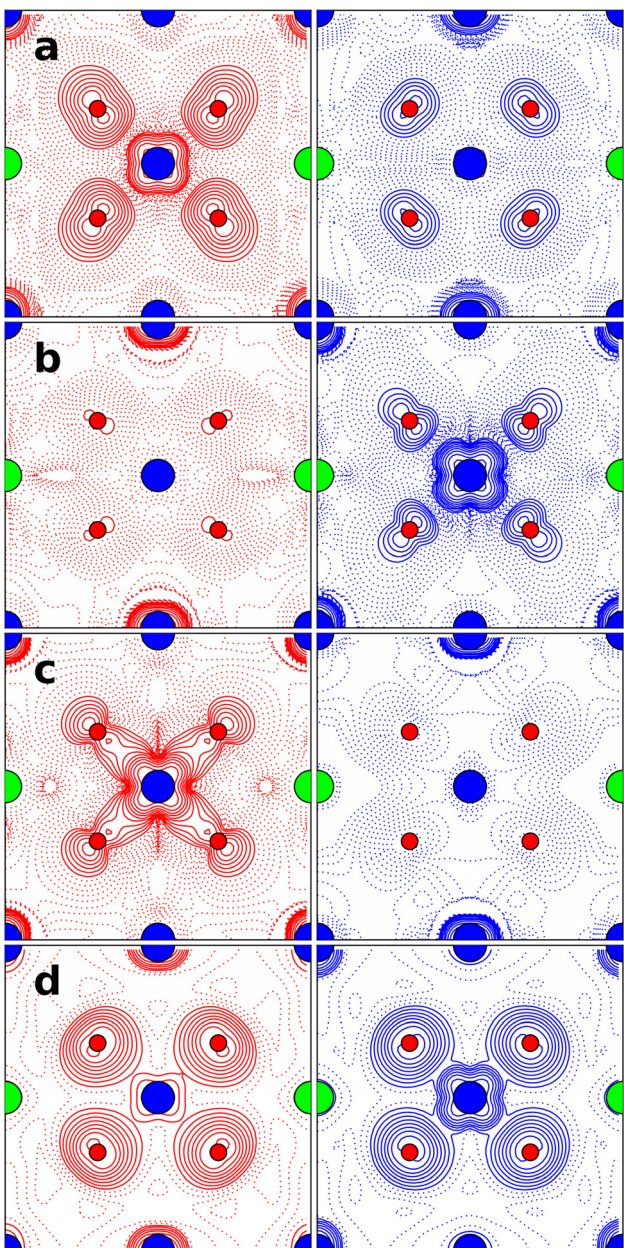


Figure S5. Spin-up (left, red) and spin-down (right, blue) electron densities of a) the three occupied states at the top of the valence band and b) the three unoccupied states forming the narrow band above the valence band which are out-of-phase combinations of Cu 3d and O 2p orbitals, c) the three occupied states just below the valence band which are in-phase combinations of Cu 3d and O 2p orbitals, d) the conduction band showing the unoccupied in-phase combinations of Cu 3d and O 2p orbitals. Densities are plotted in the $z = 0$ plane with logarithmic contours. Contours below an

arbitrary threshold are shown dashed. The positions of the calcium (green), copper (blue) and oxygen (red) atoms are included in the plots.

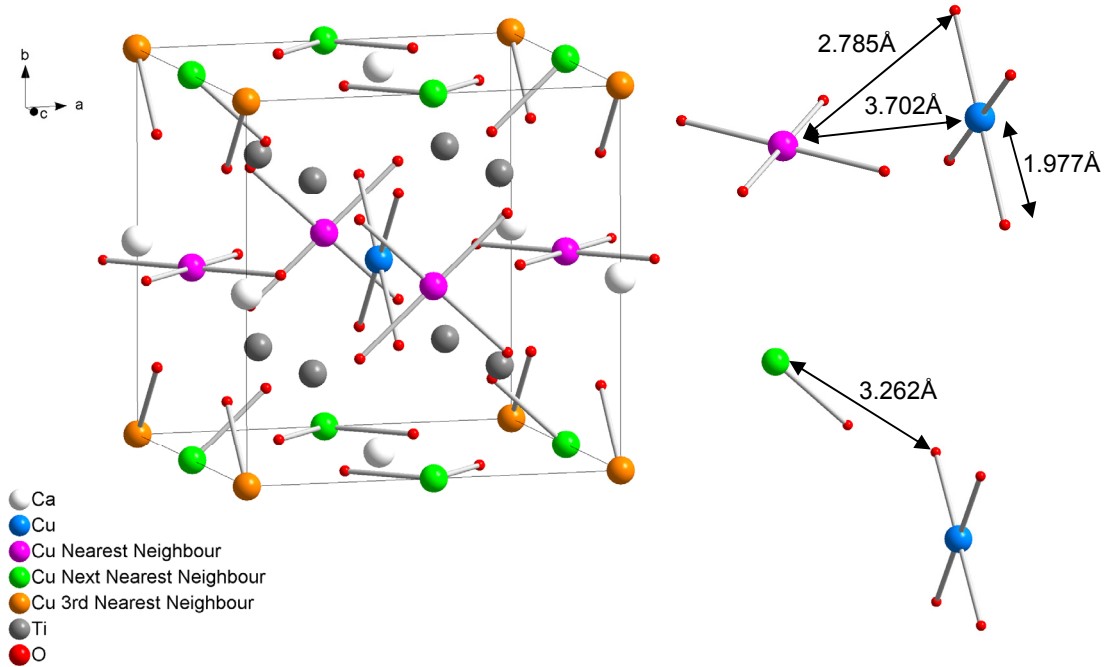


Figure S6. Unit cell structure of $\text{CaCu}_3\text{Ti}_4\text{O}_{12}$ (left) and highlighted distances (right) showing coordination and isolation of CuO_4 units

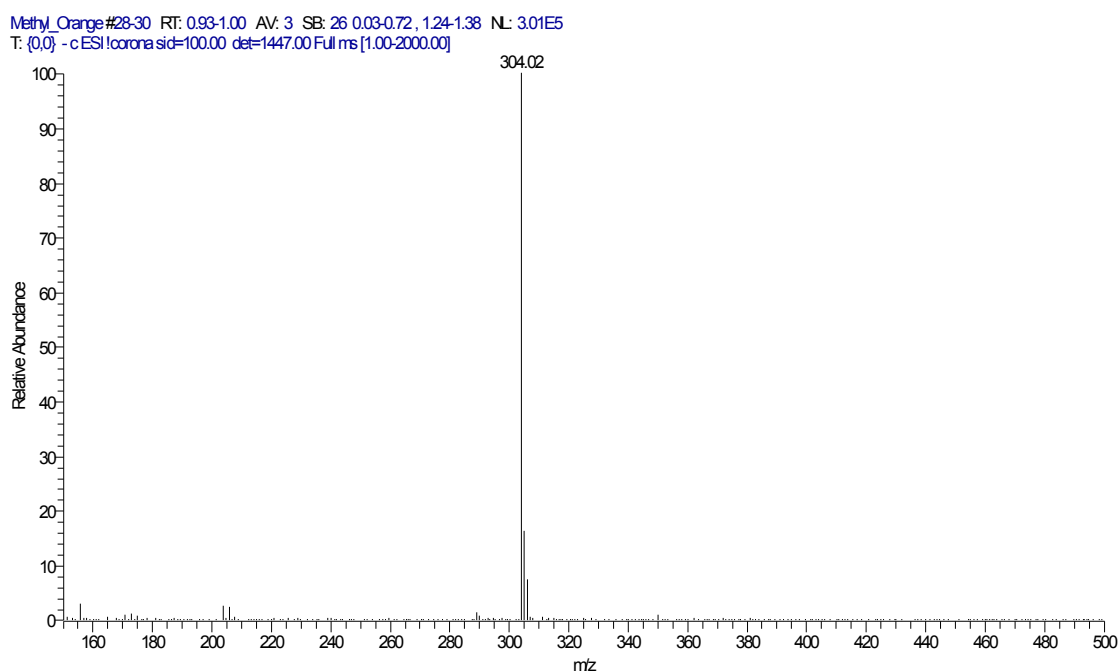


Figure S7. MS data from MO in water.

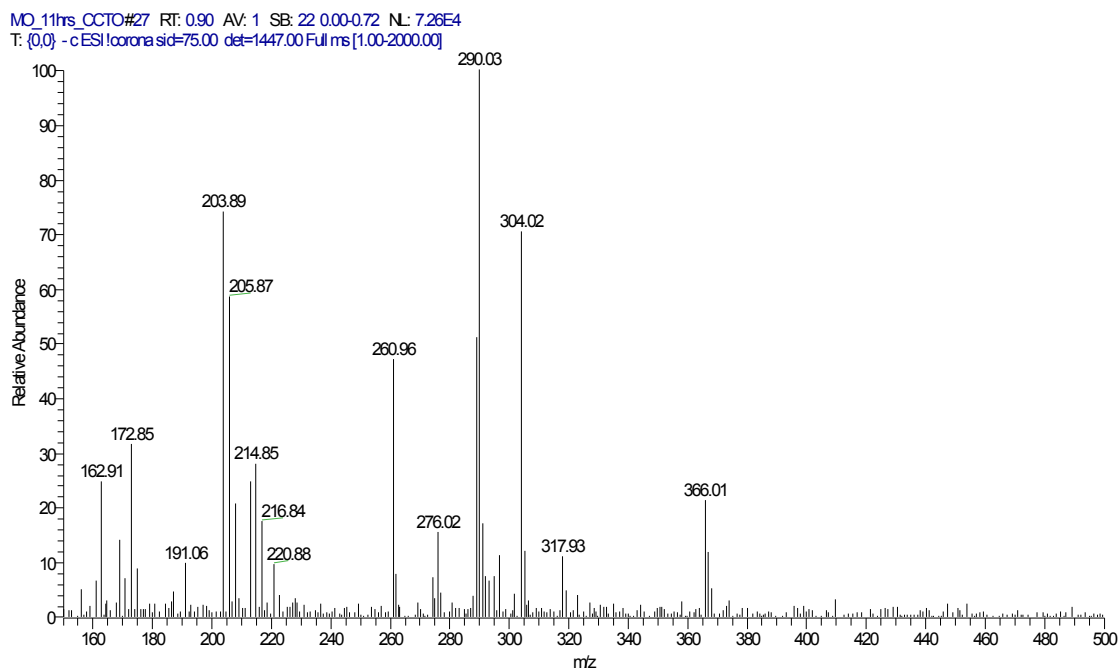


Figure S8. MS data from MO after 11hrs under visible light irradiation in the presence of Pt-
 $\text{CaCu}_3\text{Ti}_4\text{O}_{12}$.

JC4CPB#112-118 RT: 1.93-2.03 AV: 7 SB: 180 0.03-1.61 ,243-3.94 NL: 2.52E6
T: {0.0} - cESI!corona sid=50.00 det=1447.00 Full ms [1.00-2000.00]

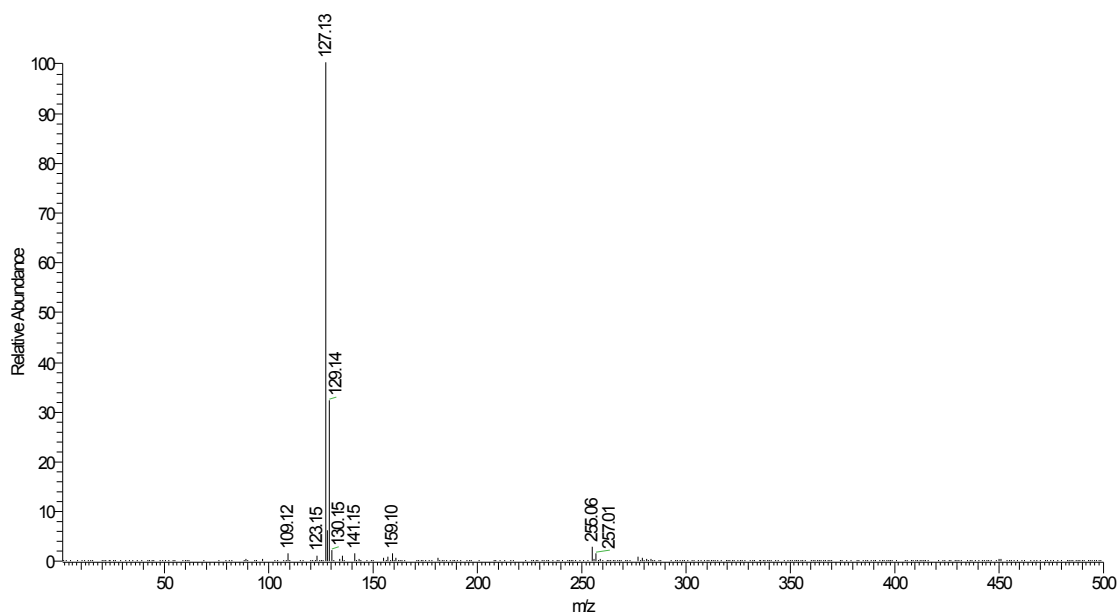


Figure S9. MS data from 4CP in water.

JCP25UV15_2in10#104-110 RT: 1.79-1.89 AV: 7 SB: 179 0.03-1.46 ,2.32-3.97 NL: 7.02E5
T: {0.0} - cESI!corona sid=50.00 det=1447.00 Full ms [1.00-2000.00]

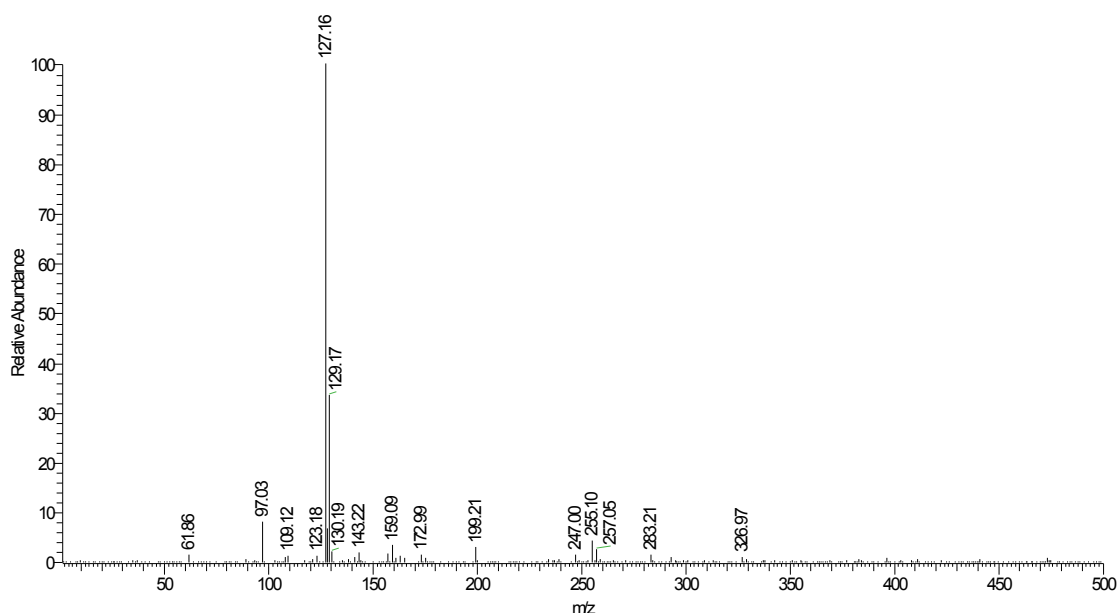


Figure S10. MS data from 4CP after 15mins under UV light irradiation in the presence of P25.

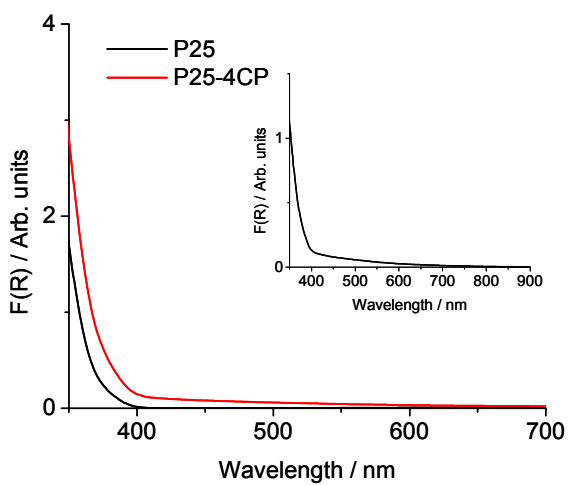


Figure S11. Diffuse reflectance spectra of TiO₂ before and after visible light irradiation in the presence of 4CP, showing visible light absorption originating from 4CP-Ti charge transfer surface complex. Inset shows difference diffuse reflectance spectrum.

JCP25UMS2_2in10#104-110 RT: 1.79-1.89 AV: 7 SB: 192.03-1.53, 2.13-3.94 NL: 7.43E5
T: {0.0} -c ESI!corona sid=50.00 det=1447.00 Full ms [1.00-2000.00]

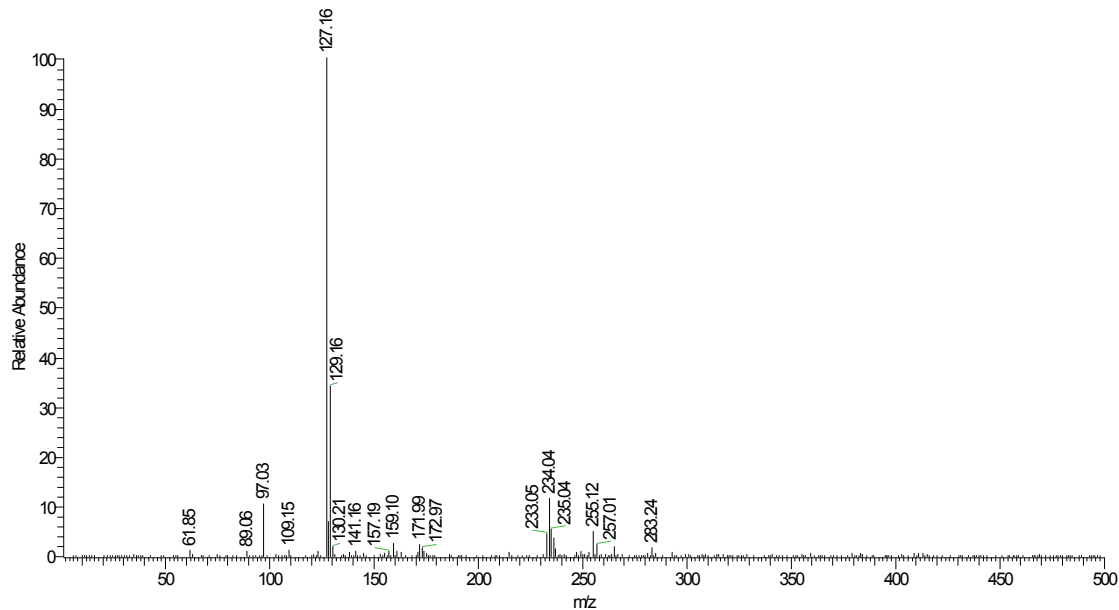


Figure S12. MS data from 4CP after 2hrs under visible light irradiation in the presence of P25.

JC4OPCCTOU1#112-117 RT: 1.93-2.01 AV: 6 SB: 177 0.05-1.61,243-3.90 NL: 1.66E6
T: {0,0} -c ESI!corona sd=50.00 det=1447.00 Full ms[1.00-2000.00]

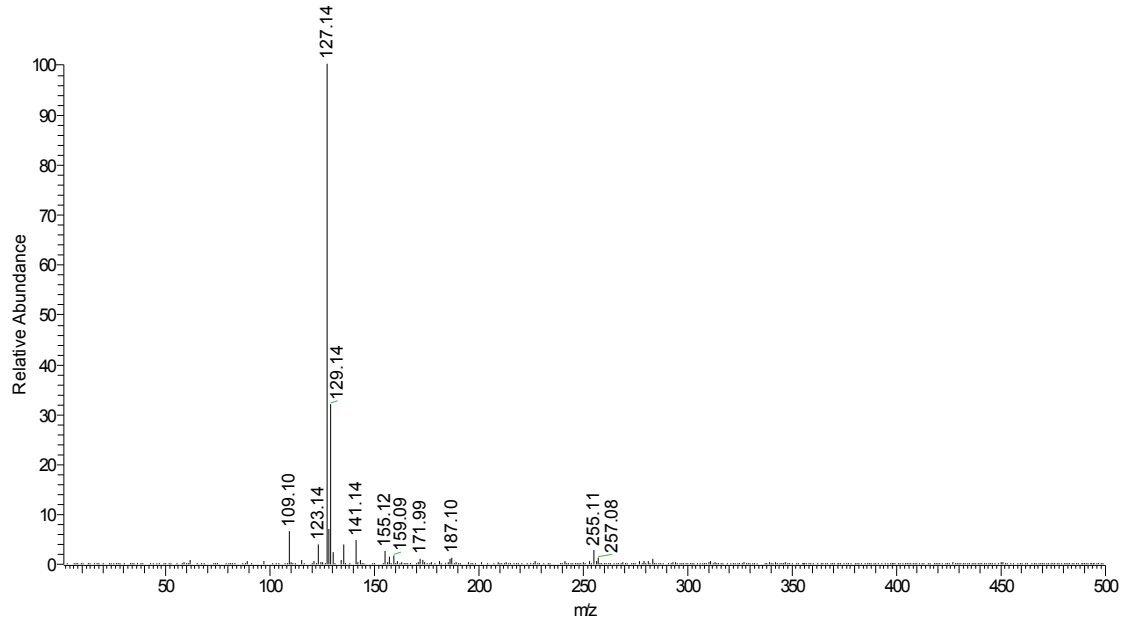


Figure S13. MS data from 4CP after 1hr UV light irradiation in the presence of Pt-CaCu₃Ti₄O₁₂.

JC4OPCCTOU5#112-117 RT: 1.93-2.01 AV: 6 SB: 178 0.02-1.58,246-3.96 NL: 8.28E5
T: {0,0} -c ESI!corona sd=50.00 det=1447.00 Full ms[1.00-2000.00]

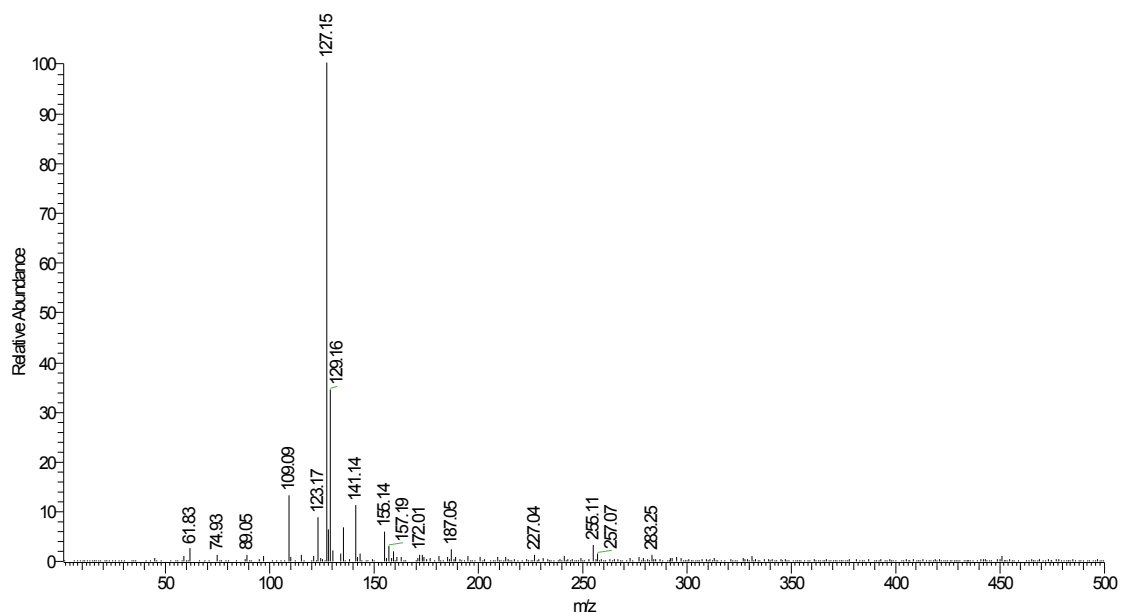


Figure S14. MS data from 4CP after 5hrs UV light irradiation in the presence of Pt-CaCu₃Ti₄O₁₂.

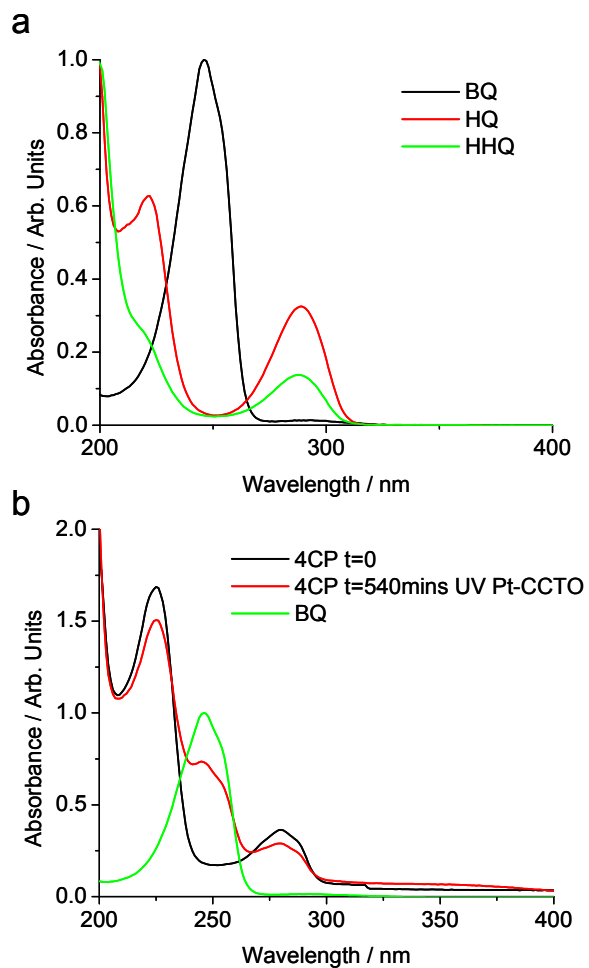


Figure S15. a) UV/Vis absorbance spectra of some key intermediates in the photo-oxidation of 4CP under UV light; **b)** comparison between the spectra of BQ and 4CP that has been photo-oxidised in the presence of Pt-CaCu₃Ti₄O₁₂.

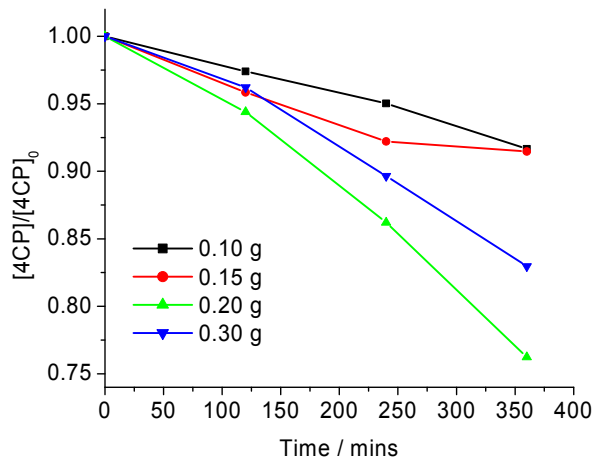


Figure S16. Normalized change in [4CP] with respect to time for 4CP+Pt-CaCu₃Ti₄O₁₂+visible light ($\lambda > 420\text{nm}$) with different amounts of catalyst present.

JC4CPOCTO12#111-118 RT: 1.91-2.03 AV: 8 SB: 189.005-1.65, 2.31-3.96 NL: 1.44E6
T: {0,0} - c ESI! corona sd=50.00 det=1447.00 Full ms [1.00-2000.00]

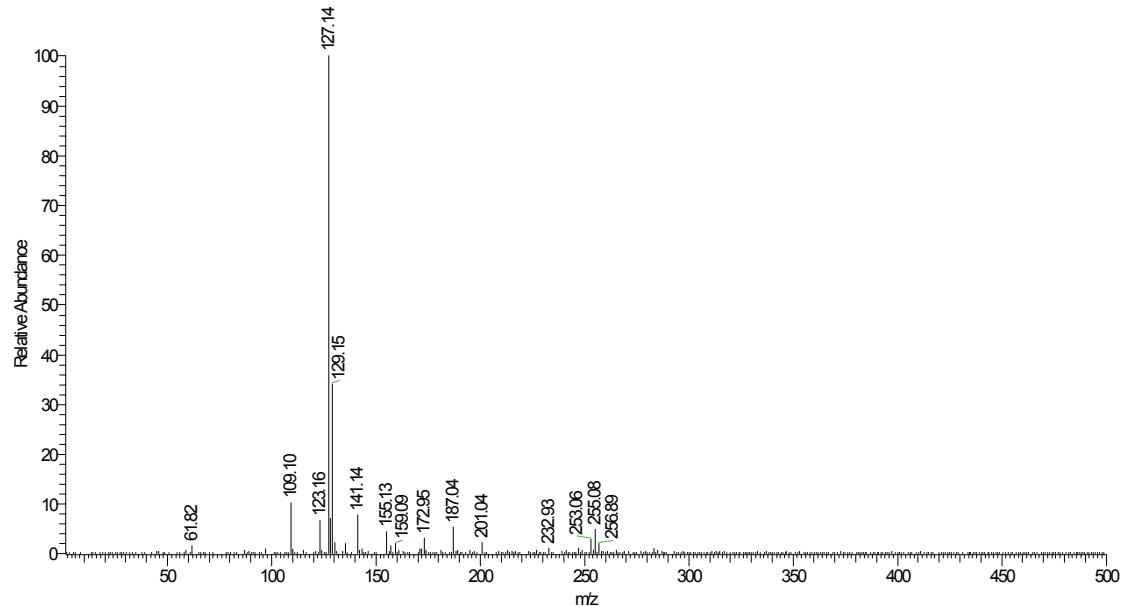


Figure S17. MS data from 4CP after 12hrs visible light irradiation in the presence of Pt-CaCu₃Ti₄O₁₂.

Estimation of Active Sites for Turnover Number Calculations for 4CP

Photo-oxidation over Pt-CaCu₃Ti₄O₁₂

0.1g 1wt%Pt-CaCu₃Ti₄O₁₂ => 0.099 x (0.1/614.184) = 1.611x10⁻⁴ mols

BET Surface Area = 11.2m²g⁻¹

CaCu₃Ti₄O₁₂ unit cell parameter a=7.393Å=7.393x10⁻¹⁰m => face area=5.46x10⁻¹⁹m²

Unit cells at surface of 1g = 11.2/5.46x10¹⁹ => 3.40x10⁻⁵ mols

=> unit cells at surface of 0.1g = 3.40x10⁻⁶ mols

1 unit cell contains 2 CaCu₃Ti₄O₁₂ => 6.8x10⁻⁶ mols at surface of 0.1g

[4CP]=0.026gL⁻¹ => 1.02x10⁻⁵ mols in 50ml

6.8x10⁻⁶ CaCu₃Ti₄O₁₂ mols at surface of 0.1g (as above)

1 turnover = 6.8x10⁻⁶/1.02x10⁻⁵ x100 = 66.66% 4CP degraded